

Kernel Methods for the Approximation of the Eigenfunctions of the Koopman Operator

Jonghyeon Lee¹, Boumediene Hamzi^{1,2}, Boya Hou³, Houman Owhadi¹,
Gabriele Santin⁴, and Umesh Vaidya⁵

¹Department of Computing and Mathematical Sciences, Caltech, CA, USA.

²Alan Turing Institute, London, UK.

³Carl R. Woese Institute for Genomic Biology, University of Illinois,
Urbana-Champaign, IL, USA.

⁴Department of Environmental Sciences, Informatics and Statistics, Ca’
Foscari University of Venice, Italy.

⁵Department of Mechanical Engineering, Clemson University, USA.

December 24, 2024

Abstract

The Koopman operator provides a linear framework to study nonlinear dynamical systems. Its spectra offer valuable insights into system dynamics, but the operator can exhibit both discrete and continuous spectra, complicating direct computations. In this paper, we introduce a kernel-based method to construct the principal eigenfunctions of the Koopman operator without explicitly computing the operator itself. These principal eigenfunctions are associated with the equilibrium dynamics, and their eigenvalues match those of the linearization of the nonlinear system at the equilibrium point. We exploit the structure of the principal eigenfunctions by decomposing them into linear and nonlinear components. The linear part corresponds to the left eigenvector of the system’s linearization at the equilibrium, while the nonlinear part is obtained by solving a partial differential equation (PDE) using kernel methods. Our approach avoids common issues such as spectral pollution and spurious eigenvalues, which can arise in previous methods. We demonstrate the effectiveness of our algorithm through numerical examples.

1 Introduction

Time series data, which are ubiquitous in various scientific domains, have driven the development of a wide range of statistical and machine learning forecasting methods [1, 2, 3, 4, 5, 6, 7, 8, 9, 10, 11, 12, 13, 14, 15, 16, 17, 18]. Dynamical

systems theory provides tools to understand the underlying rules governing the evolution of time series data. Originating with the work by Koopman [19], Koopman operator theory provides a linear lens to study nonlinear dynamical systems. In particular, the Koopman operator maps the nonlinear evolution of finite-dimensional state space to an infinite-dimensional but linear description of functions. Following the seminal work [20], there is a surge in interest in using the Koopman operator to study dynamical systems. As a linear operator, the spectral of the Koopman operator is rich in information and plays a significant role in various analysis and synthesis problems. For example, the principal eigenfunctions reveal the state space geometry as the joint zero-level curves characterize the stable and unstable manifolds of the equilibrium points [21, 22]. In [23], the principal eigenfunctions are used to identify the stability boundary, thereby determining the domain of attraction of an equilibrium point. Furthermore, the solution to the optimal control problem can also be constructed using the principal eigenfunctions of the Koopman operator, per [24, 25]. In [26], the authors proposed a path-integral formula for the computation of Koopman principal eigenfunctions. Yet in general, the Koopman operator can have both discrete and continuous spectra [20], making the computation challenging. In addition, approximating the spectra of an infinite-dimensional operator via a finite-dimensional matrix can suffer from "spectral pollution" [27]. In this paper, we aim to develop a numerical method to construct the principal eigenfunction of the Koopman operator directly from data that circumvents these difficulties.

Numerical methods such as extended dynamic mode decomposition (EDMD) [28] aim to approximate the infinite-dimensional Koopman operator via its actions on the finite-dimensional space spanned by a set of pre-selected functions. Recent research has also explored the combination of kernel methods and Koopman operator theory [29, 30, 31, 32, 33, 34]. Building upon the theory of reproducing kernel Hilbert spaces (RKHS) [35], kernel-based methods offer considerable advantages in regularization, guaranteed convergence, automatization, and interpretability [36, 37, 38, 39], and have notably strengthened the mathematical basis for analyzing dynamical systems [3, 40, 41, 42, 43, 44, 45, 29, 46, 47, 48, 49, 50, 51, 52, 53, 54, 55, 56] as well as surrogate modeling [57]. In this paper, we explore the use of kernel methods for the computation of spectral properties of the Koopman operator. The advantage of using kernel methods in this context is that they provide with error estimates that make the method more rigorous.

The existing literature on kernel-based Koopman learning, e.g. [29, 33], requires constructing a Koopman operator from data first. The spectra are then computed from the learned Koopman operator. Yet the spurious eigenvalues [58] can arise due to numerical artifacts, noise, or overfitting in the computation. These spurious eigenvalues do not represent genuine modes of the underlying dynamics and are misleading when analyzing the system's behavior. To deal with this challenge, we aim to directly learn the spectrum of the Koopman operator without computing the Koopman operator itself by solving a partial differential equation (PDE) in

RKHS. Specifically, following [26], we associate the principal eigenfunctions of the Koopman operator with an equilibrium point with the corresponding eigenvalues being the same as that of the linearization of the nonlinear system at said equilibrium point. The linear parts of the principal eigenfunction correspond to the eigenvector of local linearization at the origin, while the nonlinear part of the eigenfunction is the solution of PDEs, which can be solved in RKHS. Unlike [59] that learns eigenfunctions of the Koopman operator in RKHS, the decomposition into linear and nonlinear parts allows us to incorporate knowledge from the linearization of system dynamics, and exploit the possible nonlinear structure of RKHS.

The remainder of this paper is organized as follows: In Section 2, we provide background on the Koopman operator and its eigenfunctions. In Section 3, we discuss kernel methods and their application to solving the PDE satisfied by the Koopman eigenfunctions. Section 4 presents error estimates for our method, and in Section 5, we showcase numerical experiments.

2 Preliminaries on the Koopman Operator

2.1 Koopman Operator and its Spectrum

In this section, we provide a brief overview of the spectral theory of the Koopman operator. We refer the reader to [60, 61] for more details. Consider the dynamical system

$$\dot{x} = f(x), \tag{1}$$

defined on a state space $\mathcal{Z} \subseteq \mathbb{R}^p$. The vector field \mathbf{f} is assumed to be smooth function. Let $\mathcal{F} \subseteq \mathcal{C}^0$ be the function space of observable $\psi : \mathcal{Z} \rightarrow \mathbb{C}$. We have following definitions for the Koopman operator and its spectrum.

Definition 1 (Koopman Operator). *The family of Koopman operators $\mathbb{U}_t : \mathcal{F} \rightarrow \mathcal{F}$ corresponding to (1) is defined as*

$$[\mathbb{U}_t \psi](x) = \psi(s_t(x)). \tag{2}$$

where $s_t(x)$ is the solution of the dynamical system (1). If in addition ψ is continuously differentiable, then $\varphi(x, t) := [\mathbb{U}_t \psi](x)$ satisfies a partial differential equation [62]

$$\frac{\partial \varphi}{\partial t} = \frac{\partial \varphi}{\partial x} f =: \mathcal{K}_f \varphi \tag{3}$$

with the initial condition $\varphi(x, 0) = \psi(x)$. The operator \mathcal{K}_f is the infinitesimal generator of \mathbb{U}_t i.e.,

$$\mathcal{K}_f \psi = \lim_{t \rightarrow 0} \frac{(\mathbb{U}_t - I)\psi}{t}. \tag{4}$$

It is easy to check that each \mathbb{U}_t is a linear operator on the space of functions, \mathcal{F} .

Definition 2. [*Eigenvalues and Eigenfunctions of Koopman*] A function $\psi_\lambda(x)$, assumed to be at least C^1 , is said to be an eigenfunction of the Koopman operator associated with eigenvalue λ if

$$[\mathbb{U}_t \psi_\lambda](x) = e^{\lambda t} \psi_\lambda(x). \quad (5)$$

Using the Koopman generator, the (5) can be written as

$$\frac{\partial \psi_\lambda}{\partial x} f = \lambda \psi_\lambda. \quad (6)$$

The eigenfunctions and eigenvalues of the Koopman operator enjoy the following property [60, 63].

In this paper, we are interested in approximating the eigenfunctions of the Koopman operator with associated eigenvalues, the same as that of the linearization of the nonlinear system at the equilibrium point. With the hyperbolicity assumption on the equilibrium point of the system (1), this part of the spectrum of interest to us is well-defined. In the following discussion, we summarize the results from [60] relevant to this paper and justify some of the claims made above on the spectrum of the Koopman operator.

Equations (5) and (6) provide a general definition of the Koopman spectrum. However, the spectrum can be defined over finite time or over a subset of the state space. The spectrum of interest to us in this paper could be well-defined over the subset of the state space.

Definition 3 (Open Eigenfunction [60]). Let $\psi_\lambda : \mathcal{C} \rightarrow \mathbb{C}$, where $\mathcal{C} \subset \mathcal{Z}$ is not an invariant set. Let $x \in \mathcal{C}$, and $\tau \in (\tau^-(x), \tau^+(x)) = I_x$, a connected open interval such that $\tau(x) \in \mathcal{C}$ for all $\tau \in I_x$. If

$$[\mathbb{U}_\tau \psi_\lambda](x) = \psi_\lambda(\mathbf{s}_\tau(x)) = e^{\lambda \tau} \psi_\lambda(x), \quad \forall \tau \in I_x. \quad (7)$$

Then $\psi_\lambda(x)$ is called the open eigenfunction of the Koopman operator family \mathbb{U}_t , for $t \in \mathbb{R}$ with eigenvalue λ .

If \mathcal{C} is a proper invariant subset of \mathcal{Z} in which case $I_x = \mathbb{R}$ for every $x \in \mathcal{C}$, then ψ_λ is called the subdomain eigenfunction. If $\mathcal{C} = \mathcal{Z}$ then ψ_λ will be the ordinary eigenfunction associated with eigenvalue λ as defined in (5). The open eigenfunctions as defined above can be extended from \mathcal{C} to a larger reachable set when \mathcal{C} is open based on the construction procedure outlined in [60, Definition 5.2, Lemma 5.1]. Let \mathcal{P} be that larger domain. The eigenvalues of the linearization of the system dynamics at the origin, i.e., E , will form the eigenvalues of the Koopman operator [60, Proposition 5.8]. Our interest will be in constructing the corresponding eigenfunctions, defined over the domain \mathcal{P} . We will refer to these eigenfunctions

as *principal eigenfunctions* [60].

The principal eigenfunctions can be used as a change of coordinates in the linear representation of a nonlinear system and draw a connection to the famous Hartman-Grobman theorem on linearization and Poincare normal form [64]. The principal eigenfunctions will be defined over a proper subset \mathcal{P} of the state space \mathcal{Z} (called subdomain eigenfunctions) or over the entire \mathcal{Z} [60, Lemma 5.1, Corollary 5.1, 5.2, and 5.8].

2.2 Decomposition of Koopman Eigenfunctions

Following [26], we decompose principle eigenfunctions into linear and nonlinear parts. Specifically, consider the decomposition of the nonlinear system into linear and nonlinear parts as

$$\dot{x} = f(x) = Ex + (f(x) - Ex) =: Ex + G(x). \quad (8)$$

where $E = \frac{\partial f}{\partial x}(0)$ with Ex the linear part and G the purely nonlinear part. For the simplicity of presentation and continuity of notations, we present approximation results for eigenfunctions with simple real eigenvalues; the extension to the complex case is deferred to future work. Let λ be the eigenvalues of the Koopman generator and also of E . The eigenfunction corresponding to eigenvalue λ admits the decomposition into linear and nonlinear parts.

$$\phi_\lambda(x) = w^\top x + h(x), \quad (9)$$

where $w^\top x$ and $h(x)$ are the eigenfunction's linear and purely nonlinear parts, respectively. Substituting (9) in following general expression of Koopman eigenfunction i.e.,

$$\frac{\partial \phi_\lambda}{\partial x}(x) \cdot f(x) = \lambda \phi_\lambda(x) \quad (10)$$

and using (8), we obtain following equations to be satisfied by w and $h(x)$

$$w^\top E = \lambda w^\top, \quad \frac{\partial h}{\partial x}(x) \cdot f(x) - \lambda h(x) + w^\top G(x) = 0. \quad (11)$$

So, the linear part of the eigenfunction can be found as the left eigenvector with eigenvalue λ of the matrix E , and the nonlinear term satisfies the linear partial differential equation.

3 RKHS-based Computational Framework

3.1 Reproducing Kernel Hilbert Spaces (RKHS)

We give a brief overview of reproducing kernel Hilbert spaces as used in statistical learning theory [35]. Early work developing the theory of RKHS was undertaken by N. Aronszajn [65].

Definition 4. Let \mathcal{H} be a Hilbert space of functions on a set \mathcal{X} . Denote by $\langle f, g \rangle$ the inner product on \mathcal{H} and let $\|f\| = \langle f, f \rangle^{1/2}$ be the norm in \mathcal{H} , for f and $g \in \mathcal{H}$. We say that \mathcal{H} is a reproducing kernel Hilbert space (RKHS) if there exists a function $k : \mathcal{X} \times \mathcal{X} \rightarrow \mathbb{R}$ such that

- i. $k_x := k(x, \cdot) \in \mathcal{H}$ for all $x \in \mathcal{X}$.
- ii. k spans \mathcal{H} : $\mathcal{H} = \overline{\text{span}\{k_x \mid x \in \mathcal{X}\}}$.
- iii. k has the reproducing property: $\forall f \in \mathcal{H}, f(x) = \langle f, k_x \rangle$.

k will be called a reproducing kernel of \mathcal{H} . \mathcal{H}_k will denote the RKHS \mathcal{H} with reproducing kernel k where it is convenient to explicitly note this dependence.

The important properties of reproducing kernels are summarized in the following proposition.

Proposition 1. [65] If k is a reproducing kernel of a Hilbert space \mathcal{H} , then

- i. $k(x, y)$ is unique.
- ii. $\forall x, y \in \mathcal{X}, k(x, y) = k(y, x)$ (symmetry).
- iii. $\sum_{i,j=1}^q \alpha_i \alpha_j k(x_i, x_j) \geq 0$ for $\alpha_i \in \mathbb{R}, x_i \in \mathcal{X}$ and $q \in \mathbb{N}_+$ (positive definiteness).
- iv. $\langle k(x, \cdot), k(y, \cdot) \rangle = K(x, y)$.

Common examples of reproducing kernels defined on a compact domain $\mathcal{X} \subset \mathbb{R}^n$ are the (1) constant kernel: $K(x, y) = m > 0$ (2) linear kernel: $k(x, y) = x \cdot y$ (3) polynomial kernel: $k(x, y) = (1 + x \cdot y)^d$ for $d \in \mathbb{N}_+$ (4) Laplace kernel: $k(x, y) = e^{-\|x-y\|_2/\sigma^2}$, with $\sigma > 0$ (5) Gaussian kernel: $k(x, y) = e^{-\|x-y\|_2^2/\sigma^2}$, with $\sigma > 0$ (6) triangular kernel: $k(x, y) = \max\{0, 1 - \frac{\|x-y\|_2^2}{\sigma}\}$, with $\sigma > 0$. (7) locally periodic kernel: $k(x, y) = \sigma^2 e^{-2\frac{\sin^2(\pi\|x-y\|_2/p)}{\ell^2}} e^{-\frac{\|x-y\|_2^2}{2\ell^2}}$, with $\sigma, \ell, p > 0$.

Theorem 1. [65] Let $k : \mathcal{X} \times \mathcal{X} \rightarrow \mathbb{R}$ be a symmetric and positive definite function. Then there exists a Hilbert space of functions \mathcal{H} defined on \mathcal{X} admitting k as a reproducing Kernel. Conversely, let \mathcal{H} be a Hilbert space of functions $f : \mathcal{X} \rightarrow \mathbb{R}$ satisfying $\forall x \in \mathcal{X}, \exists \kappa_x > 0$, such that $|f(x)| \leq \kappa_x \|f\|_{\mathcal{H}}, \forall f \in \mathcal{H}$. Then \mathcal{H} has a reproducing kernel k .

Theorem 2. [65] Let $k(x, y)$ be a positive definite kernel on a compact domain or a manifold X . Then there exists a Hilbert space \mathcal{F} and a function $\Phi : X \rightarrow \mathcal{F}$ such that

$$k(x, y) = \langle \Phi(x), \Phi(y) \rangle_{\mathcal{F}} \quad \text{for } x, y \in X.$$

Φ is called a feature map, and \mathcal{F} a feature space¹.

Theorem 2 is often referred to as the “kernel trick”, and its utility lies in the fact that the kernel function obviates the need to compute high-dimensional outputs of the feature map Φ directly.

Theorem 3. [66] Let $k : X \times X \rightarrow \mathbb{R}$ be a real-valued kernel and K be the associated RKHS of functions mapping X to \mathbb{R} . Let $\Phi = (\Phi_1, \dots, \Phi_n) \in (K^*)^n$ be a vector of linear functionals from K to \mathbb{R} , and write $\Phi(u) = ([\Phi_1, u], \dots, [\Phi_n, u]) \in \mathbb{R}^n$, where $[\cdot, \cdot]$ is the dual pairing. Then for $y \in \mathbb{R}^n$,

$$\operatorname{argmin}_{u \in \mathcal{H}_K \text{ s.t. } \Phi(u)=y} \|u\|_K = \mathbb{E}[\xi | \Phi(\xi) = y]. \quad (12)$$

Here, ξ is a centered Gaussian process with covariance $K : \mathcal{B} \rightarrow \mathcal{B}^*$, where \mathcal{B} is a separable Banach space, which is a linear bijection that is symmetric ($[\phi, K\varphi] = [\varphi, K\phi]$) and positive ($[\phi, K\phi] > 0$ for $\phi \neq 0$).

Theorem 3 is significant because it states that the problem of recovering a sufficiently regular function u with respect to constraints $\Phi(u) = y$ is equivalent to finding the conditional expectation of ξ , the Gaussian process approximation of u , given observations $\Phi(\xi) = y$. Fortunately, (3) has a closed-form solution given in the theorem below:

Theorem 4. [66] The conditional expectation of a Gaussian process ξ in \mathcal{B} given observations $\Phi(u)$ is given by the following representer formula:

$$\mathbb{E}[\xi | \Phi(u) = y] = \sum_{i,j=1}^m [\Phi_i, \xi] \Theta_{i,j}^{-1} T\Phi_j \in \mathcal{B} \quad (13)$$

We outline the key steps in proving Theorem (4) and refer interested readers to [66] for details. Consider the conditional expectation of $[\xi, \psi]$ given $\Phi(u)$, where ψ is an arbitrary element of the dual Banach space \mathcal{B}^* . Since $[\xi, \psi] \in \mathbb{R}$ is a real-valued Gaussian variable, we may use results from classical probability theory to show that $\mathbb{E}[[\psi, \xi] | \Phi(u)] = \sum_{i=1}^m c_i [\Phi_i, \xi]$, where c_i are coefficients that satisfy $[\psi, \xi] - \sum_{i=1}^m c_i [\Phi_i, \xi]$ are independent from $[\Phi_j, \xi] \forall j$. This in turn implies that $\operatorname{Cov}[[\psi, \xi] - \sum_{i=1}^m c_i [\Phi_i, \xi], [\Phi_j, \xi]] = 0 \Leftrightarrow [\psi, T\Phi_j] - \sum_{i=1}^m c_i [\Phi_i, T\Phi_j] = 0$. Now define Θ to be an $m \times m$ matrix with entries $\Theta_{i,j} = [\Phi_i, T\Phi_j]$, which is equivalent to stating that $[\psi, T\Phi_j] = \sum_{i=1}^m c_i \Theta_{i,j}$. If Θ is invertible, $c_i = \sum_{j=1}^m \Theta_{i,j}^{-1} [\psi, T\Phi_j]$. Therefore, we have

$$\mathbb{E}[[\psi, \xi] | [\Phi_1, \xi], \dots, [\Phi_m, \xi]] = \sum_{i,j=1}^m [\Phi_i, \xi] \underbrace{\Theta_{i,j}^{-1}}_{\in \mathcal{B}} T\Phi_j = [\psi, \sum_{i,j=1}^m [\Phi_i, \xi] \Theta_{i,j}^{-1} T\Phi_j]. \quad (14)$$

¹The dimension of the feature space can be infinite, for example in the case of the Gaussian kernel.

Since this is true for all $\psi \in \mathcal{B}^*$, we conclude that

$$\mathbb{E}[\xi[[\Phi_1, \xi], \dots, [\Phi_m, \xi]]] = \sum_{i,j=1}^m [\Phi_i, \xi] \Theta_{i,j}^{-1} T \Phi_j \in \mathcal{B}. \quad (15)$$

In the next section, we write the generalized representer formula (15) in the equivalent form

$$u(\cdot) = K(\cdot, \tilde{\phi}) K(\tilde{\phi}, \tilde{\phi})^{-1} Y, \quad (16)$$

where $K(\tilde{\phi}, \tilde{\phi}) = \Theta$, $Y_i = [\tilde{\phi}_i, \xi]$ and $K(\cdot, \tilde{\phi}_i) = T \tilde{\phi}_i$

3.2 Solving the linear PDE from data

Solving the linear PDE (11) can be framed as a quadratic optimization problem which can be solved by kernel regression. For each eigenvalue λ_k , $k = 1, \dots, n$, define the best Gaussian approximation of h_{λ_k} , where h_{λ_k} is a function of d variables, to be the $h_{\lambda_k}^*$ that satisfies

$$\begin{aligned} \min_{h_{\lambda_k}^* \in \mathcal{H}_K} \quad & \|h_{\lambda_k}^*\|_K^2 \\ \text{s.t.} \quad & h_{\lambda_k}^*(\mathbf{0}) = 0 \\ & \frac{\partial}{\partial z_j} h_{\lambda_k}^*(\mathbf{0}) = 0, \quad j = 1, \dots, d \\ & \frac{\partial h_{\lambda_k}^*}{\partial \mathbf{z}}(\mathbf{z}_i) \cdot \mathbf{F}(\mathbf{z}_i) - \lambda_k h_{\lambda_k}^*(\mathbf{z}_i) = -\mathbf{w}_k^T \mathbf{G}(\mathbf{z}_i), \quad i = 1, \dots, N \end{aligned} \quad (17)$$

where $\mathbf{z}_i := (z_{1,i}, z_{2,i}, \dots, z_{d,i})$ denotes our collocation points.

Define

$$\begin{aligned} \tilde{\phi}_1(\mathbf{z}) &= \delta_{\mathbf{0}}(\mathbf{z}), \\ \tilde{\phi}_{1+i}(\mathbf{z}) &= \delta_{\mathbf{0}}(\mathbf{z}) \cdot \frac{\partial}{\partial z_i}, \quad i = 1, \dots, d, \\ \tilde{\phi}_{1+d+i}(\mathbf{z}) &= \sum_{j=1}^d F(\mathbf{z}_i)_j \delta_{\mathbf{z}_i}(\mathbf{z}) \cdot \frac{\partial}{\partial z_j} - \lambda_k \delta_{\mathbf{z}_i}(\mathbf{z}), \quad i = 1, \dots, N, \end{aligned} \quad (18)$$

where $\delta_{\mathbf{z}_i}(\mathbf{z})$ is the Dirac delta distribution centered at \mathbf{z}_i .

Then the optimization problem (17) has an explicit solution given by the representer formula

$$h_k^*(\mathbf{z}) = K(\mathbf{z}, \tilde{\phi}) (K(\tilde{\phi}, \tilde{\phi}) + \eta I)^{-1} Y, \quad (19)$$

where $K(\mathbf{z}, \tilde{\phi})$ is a vector of length $N + d + 1$ with entries

$$K(\mathbf{z}, \tilde{\phi})_i := [K(\mathbf{z}, \cdot), \phi_i] = \int_{\mathbb{R}^d} K(\mathbf{z}, \mathbf{z}') \tilde{\phi}_i(\mathbf{z}') d\mathbf{z}', \quad (20)$$

and $K(\tilde{\phi}, \tilde{\phi})$ is a $(N + d + 1) \times (N + d + 1)$ matrix with entries

$$K(\tilde{\phi}_i, \tilde{\phi}_j) := \int_{\mathbb{R}^{2d}} \tilde{\phi}_i(\mathbf{z}) K(\mathbf{z}, \mathbf{z}') \tilde{\phi}_j(\mathbf{z}') d\mathbf{z} d\mathbf{z}', \quad (21)$$

and $Y \in \mathbb{R}^{N+d+1}$ is a vector with entries $Y_1 = \dots = Y_{d+1} = 0$ and $Y_{d+1+i} = -\mathbf{G}(\mathbf{z}_i)^T \mathbf{w}_k$, $i = 1, \dots, N$. η is a small positive regularization constant that reduces numerical errors associated with inverting the matrix $K(\tilde{\phi}, \tilde{\phi})$.

4 Error Estimates

Theorem 5 (Validity of Stability and Smoothness Assumptions). *Let the equilibrium point x_e of the ODE (1) be hyperbolic. Assume that $f \in C^m(\Omega, \mathbb{R}^d)$ for some integer $m \geq 1$, where Ω is an open neighborhood around x_e .*

Let $\mathbf{w} \in \mathbb{R}^d$ be a fixed weight vector. Consider the partial differential equation (PDE)

$$Dh(x) := \nabla h(x) \cdot f(x) - \lambda h(x) = -\mathbf{w}^\top G(x), \quad x \in \Omega, \quad (22)$$

with boundary conditions

$$h(x_e) = 0, \quad \nabla h(x_e) = 0. \quad (23)$$

Then, the solution $h(x)$ satisfies:

1. $h(x) \in W_2^{m+1}(\Omega)$, i.e., $h(x)$ belongs to the Sobolev space $W_2^{m+1}(\Omega)$.
2. There exists a stability bound of the form

$$\|h\|_{L_p(\Omega)} \leq C_D \|Dh\|_{L_q(\Omega)} + C_0 |h(x_e)| + C'_0 \|\nabla h(x_e)\|_{\ell^r}, \quad (24)$$

where $C_D, C_0, C'_0 > 0$ are constants, and $p, q, r \in [1, \infty]$.

Proof. We first observe that the nonlinear term $G(x) = f(x) - Ex$, where $E = \left. \frac{\partial f}{\partial x} \right|_{x_e}$, has smoothness $G(x) \in C^m(\Omega, \mathbb{R}^d)$.

Step 1: Injectivity of D

Since x_e is hyperbolic, the Jacobian matrix E has no eigenvalues with zero real parts. This implies that the linearized system around x_e has no neutral modes, and thus the operator D associated with the PDE has no non-trivial solutions to the homogeneous equation $Dh = 0$.

By the Hartman-Grobman theorem, the behavior of the nonlinear system near x_e is qualitatively similar to its linearization. Therefore, the vector field $f(x)$ can be approximated by $f(x) \approx E(x - x_e)$ near x_e , and the operator D reduces to a linear problem in this neighborhood. The only solution to $Dh = 0$ near x_e is the trivial solution $h(x) = 0$.

Thus, D is injective:

$$\ker(D) = \{h \in W_2^{m+1}(\Omega) \mid Dh = 0\} = \{0\}.$$

Step 2: Surjectivity of D

To prove surjectivity, consider the equation:

$$Dh(x) = -\mathbf{w}^\top G(x),$$

where $G(x) \in \mathcal{C}^m(\Omega)$. The solution to this equation is governed by regularity theory of Elliptic PDEs. Specifically, for smooth forcing terms $G(x)$, elliptic regularity guarantees that the operator D will have a solution in the Sobolev space $W_2^{m+1}(\Omega)$, i.e., $h(x) \in W_2^{m+1}(\Omega)$.

Elliptic regularity theory ensures that if the right-hand side $-\mathbf{w}^\top G(x)$ is sufficiently smooth, the solution $h(x)$ will also be smooth and lie in $W_2^{m+1}(\Omega)$. Therefore, D is surjective, meaning that for any smooth $G(x)$, there exists a solution $h(x) \in W_2^{m+1}(\Omega)$.

Step 3: Bounded Invertibility via the Banach Inverse Mapping Theorem

Since D is a bounded linear operator (under the smoothness and boundedness assumptions on $f(x)$ and λ) that is both injective and surjective, it is a bounded linear bijection between $W_2^{m+1}(\Omega)$ and $L_q(\Omega)$.

By the Banach Inverse Mapping Theorem, the inverse operator D^{-1} exists and is bounded. Therefore, there exists a constant $C_D > 0$ such that:

$$\|h\|_{W_2^{m+1}(\Omega)} \leq C_D \|Dh\|_{L_q(\Omega)}$$

Step 4: Stability Bound for $h(x)$

The solution $h(x)$ lies in the Sobolev space $W_2^{m+1}(\Omega)$, and we apply Sobolev embedding theorems to obtain a bound for $h(x)$ in $L_p(\Omega)$. Sobolev embedding states that for an embedding $W_2^{m+1}(\Omega) \subset L_p(\Omega)$, the solution $h(x)$ will be in $L_p(\Omega)$ for some p , provided that m is large enough.

The stability bound is expressed as:

$$\|h\|_{L_p(\Omega)} \leq C_D \|Dh\|_{L_q(\Omega)} + C_0 |h(x_e)| + C'_0 \|\nabla h(x_e)\|_{\ell^r}.$$

This bound reflects the control over $h(x)$ both in terms of the forcing term $G(x)$ (through the L_q -norm of $Dh(x)$) and the boundary conditions $h(x_e)$ and $\nabla h(x_e)$. □

To formulate the following convergence result we make use of the fill distance $\rho_{Z,\Omega}$ of the finite set $Z \subset \Omega$, given by

$$\rho_{Z,\Omega} := \sup_{x \in \Omega} \min_{z \in Z} \|x - z\|_2.$$

Theorem 6. Assume that Theorem 5 holds with constants $m > d/2$, $p, q \in [1, \infty]$, $C_D > 0$, and let h_λ be the solution of the PDE (22). Assume furthermore that $\mathcal{H} \hookrightarrow W_2^{m+1}(\Omega)$, and let h_λ^* be the solution of the corresponding optimization problem (17) with collocation points $Z \subset \Omega$ and with no regularization (i.e., $\eta = 0$ in (19)).

Then there are constants $\rho, C > 0$ depending on d, m, Ω, p, q , but not on λ, f, Z, h_λ , such that if $\rho_{Z, \Omega} < \rho_0$ it holds

$$\|h_\lambda - h_\lambda^*\|_{L_p(\Omega)} \leq C \left(\|f\|_{W_2^m(\Omega, \mathbb{R}^d)} + |\lambda| \right) \rho_{Z, \Omega}^{m-d\left(\frac{1}{2}-\frac{1}{q}\right)_+} \|h_\lambda\|_K,$$

where $(x)_+ := \max(x, 0)$.

Proof. We first show that $h \in W_2^{m+1}(\Omega)$ implies that $Dh \in W_2^m(\Omega)$, and give an estimate on its norm. Namely, for any $\alpha \in \mathbb{N}_0^d$ with $|\alpha| \leq m$ we have

$$\begin{aligned} \partial^\alpha Dh(z) &= \partial^\alpha (f(z)^T \nabla h(z) - \lambda h(z)) \\ &= \sum_{i=1}^d (\partial^\alpha f_i(z)) (\nabla h(z))_i + \sum_{i=1}^d f_i(z) \partial^\alpha (\nabla h(z))_i - \lambda \partial^\alpha h(z), \end{aligned}$$

and thus there is a constant C_d depending on d such that

$$\begin{aligned} \|\partial^\alpha Dh(z)\|_{L_2} &\leq d \max_{1 \leq i \leq d} (\|\partial^\alpha f_i\|_{L_2} \|(\nabla h)_i\|_{L_2} + \|f_i\|_{L_2} \|\partial^\alpha (\nabla h)_i\|_{L_2}) + |\lambda| \|\partial^\alpha h\|_{L_2} \\ &\leq C_d \left(\|f\|_{W_2^m(\Omega, \mathbb{R}^d)} + |\lambda| \right) \|h\|_{W_2^{m+1}}. \end{aligned}$$

This in turns implies that for some constant $C_{d,m} > 0$ depending on d and m we have

$$\|Dh\|_{W_2^m} = \left(\sum_{|\alpha| \leq m} \|\partial^\alpha Dh\|_{L_2}^2 \right)^{1/2} \leq C_{d,m} \left(\|f\|_{W_2^m(\Omega, \mathbb{R}^d)} + |\lambda| \right) \|h\|_{W_2^{m+1}}. \quad (25)$$

This proves in particular that $Dh_\lambda^* \in W_2^m(\Omega)$ since $h_\lambda^* \in \mathcal{H} \hookrightarrow W_2^{m+1}$, while $Dh_\lambda \in W_2^{m+1}(\Omega)$ by assumption and by Theorem 5.

Since $m > d/2$, we may now use the zero lemma of Theorem 12 in [67], stating that there are $\rho_0, C > 0$, depending on Ω, p, q , such that if $\rho_{Z, \Omega} < \rho_0$ it holds

$$\|Dh_\lambda - Dh_\lambda^*\|_{L_q(\Omega)} \leq C \rho_{Z, \Omega}^{m-d\left(\frac{1}{2}-\frac{1}{q}\right)_+} \|Dh_\lambda - Dh_\lambda^*\|_{W_2^m(\Omega)}, \quad (26)$$

and using the linearity of D and the bound (25) this gives

$$\|Dh_\lambda - Dh_\lambda^*\|_{L_q} \leq C C_{d,m} \left(\|f\|_{W_2^m(\Omega, \mathbb{R}^d)} + |\lambda| \right) \rho_{Z, \Omega}^{m-d\left(\frac{1}{2}-\frac{1}{q}\right)_+} \|h_\lambda - h_\lambda^*\|_{W_2^{m+1}}. \quad (27)$$

We conclude by bounding the norm in the right-hand side. Since h_λ satisfies the constraints of the problem (17), and h_λ^* is its minimal norm solution, we have $\|h_\lambda^*\|_K \leq$

$\|h_\lambda\|_K$. Furthermore, by assumption there is $C_e > 0$ such that $\|h\|_{W_2^{m+1}} \leq C_e \|h\|_K$ for all $h \in \mathcal{H}$. It follows that

$$\|h_\lambda - h_\lambda^*\|_{W_2^{m+1}} \leq C_e \|h_\lambda - h_\lambda^*\|_K \leq C_e (\|h_\lambda\|_K + \|h_\lambda^*\|_K) \leq 2C_e \|h_\lambda\|_K,$$

and thus (27) simplifies to

$$\|Dh_\lambda - Dh_\lambda^*\|_{L^q} \leq 2CC_{d,m}C_e \left(\|f\|_{W_2^m(\Omega, \mathbb{R}^d)} + |\lambda| \right) \rho_{Z, \Omega}^{m-d\left(\frac{1}{2}-\frac{1}{q}\right)_+} \|h_\lambda\|_K.$$

Inserting this inequality in the stability bound (24) gives the result with an appropriate constant $C > 0$, since both h_λ and h_λ^* satisfy the boundary conditions (23). \square

Remark 1. *We point out that in Theorem 6 the factor $(1/2 - 1/q)_+$ is decreasing in q and vanishes for $1 \leq q \leq 2$. It follows that, given a target p , one should choose the smallest q such that (24) holds.*

5 Examples

5.1 First Analytical Example

Consider the following dynamical system with an equilibrium point at the origin.

$$\dot{x} = \begin{bmatrix} -2\lambda_2 x_2 (x_1^2 - x_2 - 2x_1 x_2^2 + x_2^4) + \lambda_1 (x_1 + 4x_1^2 x_2 - x_2^2 - 8x_1 x_2^3 + 4x_2^5) \\ 2\lambda_1 (x_1 - x_2^2)^2 - \lambda_2 (x_1^2 - x_2 - 2x_1 x_2^2 + x_2^4) \end{bmatrix}. \quad (28)$$

The eigenvalues of the linearization of the system at the origin i.e., E are $\lambda_1 = -1$ and $\lambda_2 = 3$. For this example, the principal eigenfunctions can be computed analytically and are as follows:

$$\begin{aligned} \phi_{\lambda_1}(x) &= x_1 - x_2^2, & \lambda_1 &= -1 \text{ and} \\ \phi_{\lambda_2}(x) &= -x_1^2 + x_2 + 2x_1 x_2^2 - x_2^4, & \lambda_2 &= 3. \end{aligned}$$

Using 3600 points over the square $[-1, 1] \times [-1, 1]$, we apply kernel regression with the 2D Gaussian kernel

$$K(x_1, x_2; \sigma, \sigma_2) = \exp\left(-\frac{(x_1 - y_1)^2}{2\sigma_1^2} - \frac{(x_2 - y_2)^2}{2\sigma_2^2}\right) \quad (29)$$

to learn the eigenfunction ϕ_{λ_k} and depict the results in (1) and (2). For ϕ_{λ_1} , we take $\sigma_1 = \sigma_2 = 2$; for ϕ_{λ_2} , we use $\sigma_1 = 2$ and $\sigma_2 = 3$. The pointwise relative error is very low with the exception of the points where the true solution is equal to zero.

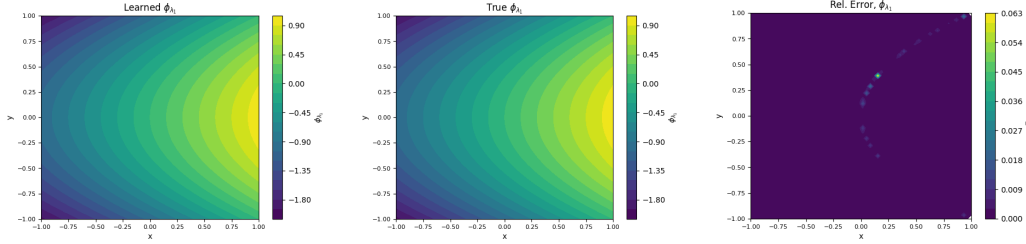


Figure 1: Learned $\phi_{\lambda_1}^*$ (left), true ϕ_{λ_1} (center) and relative error (right)

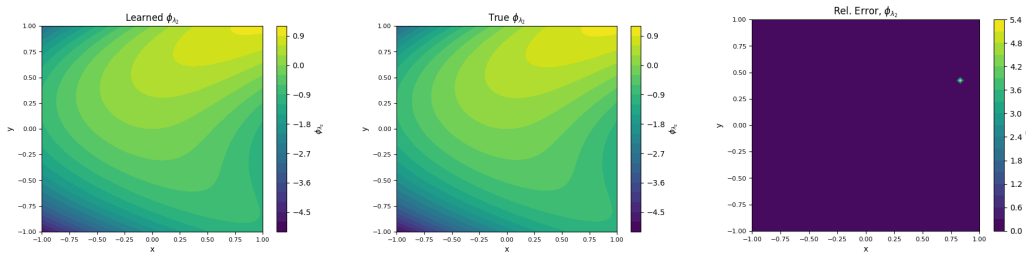


Figure 2: Learned $\phi_{\lambda_2}^*$ (left), true ϕ_{λ_2} (center) and relative error (right)

5.2 Second Analytical Example

$$\dot{x} = \begin{bmatrix} \frac{(7.5x_2^2+5.0)(x_1^3+x_1+\sin(x_2))+(-x_1+x_2^3+2x_2)\cos(x_2)}{9x_1^2x_2^2+6x_1^2+3x_2^2+\cos(x_2)+2} \\ \frac{2.5x_1^3+2.5x_1-(3x_1^2+1)(-x_1+x_2^3+2x_2)+2.5\sin(x_2)}{9x_1^2x_2^2+6x_1^2+3x_2^2+\cos(x_2)+2} \end{bmatrix}. \quad (30)$$

The vector field for this system is smooth everywhere on \mathbb{R}^2 , with a saddle point at the origin. One can verify that the two principal eigenpairs of this system are given by

$$\begin{aligned} \phi_{\lambda_1}(x) &= x_1 - 2x_2 - x_2^3, & \lambda_1 &= -1 \text{ and} \\ \phi_{\lambda_2}(x) &= x_1 + \sin(x_2) + x_1^3, & \lambda_2 &= 2.5. \end{aligned}$$

We apply the method outlined in Section 3.2 and use the 2D Gaussian kernel to solve the PDE for each eigenvalue over 2500 points in the grid $[1.5, 2.5] \times [1.5, 2.5]$,

For λ_1 , we set $\sigma_1 = \sigma_2 = 3$ and for λ_2 , we use $\sigma_1 = \sigma_2 = 7$. As shown by Figures 3 and 4, the solution $\phi_{\lambda_k}^*$, where the nonlinear part $h_{\lambda_l}^*$ has been recovered by the Gaussian kernel, is an accurate approximation of the true eigenfunction ϕ_{λ_k} for both eigenvalues λ_k .

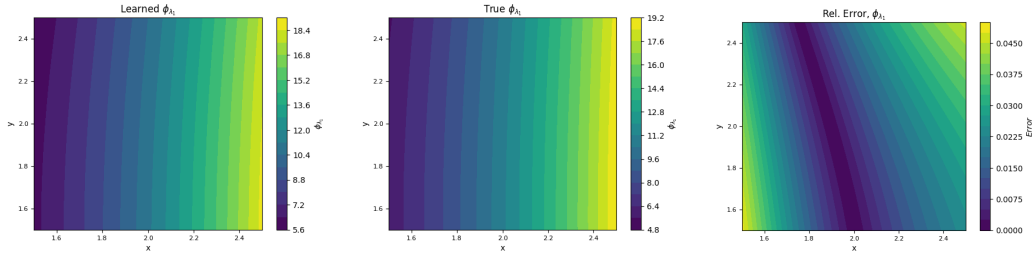


Figure 3: Learned $\phi_{\lambda_1}^*$ (left), true ϕ_{λ_1} (center) and relative error (right)

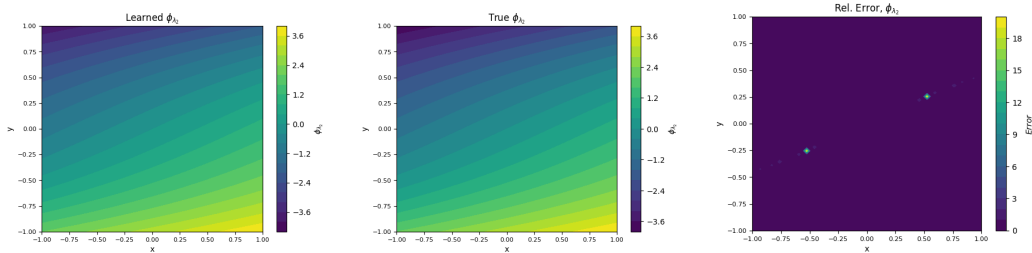


Figure 4: Learned $\phi_{\lambda_2}^*$ (left), true ϕ_{λ_2} (center) and relative error (right)

5.3 The Duffing Oscillator

Consider the unforced Duffing oscillator, described by

$$\begin{aligned}\dot{x}_1 &= x_2 \\ \dot{x}_2 &= -\delta x_2 - x_1(\beta + \alpha x_1^2)\end{aligned}\tag{31}$$

with $\delta = 0.5$, $\beta = -1$, and $\alpha = 1$, where $z \in \mathbb{R}$ and $\dot{z} \in \mathbb{R}$ are the scalar position and velocity, respectively. The dynamics admit two stable equilibrium points at $(-1, 0)$ and $(1, 0)$, and one unstable equilibrium point at the origin. In this example, we sample 2500 points over the domain $[-2, 2] \times [-2, 2]$ and use the 2D Gaussian kernel with $\sigma_1 = \sigma_2 = 15$. Our results in Figure 5 depict $\phi_{\lambda_1}^*$ for $\lambda_1 = \frac{-1 + \sqrt{17}}{4}$; this time, we consider only the larger eigenvalue. The plot accurately captures the behavior of the eigenfunction of the Koopman operator corresponding to λ_1 up to scaling.

5.4 A Three Dimensional Gradient System

Consider a three-dimensional gradient system of the form

$$\dot{x} = -\frac{\partial V}{\partial x}, \quad x = (x_1 \ x_2 \ x_3)^\top,\tag{32}$$

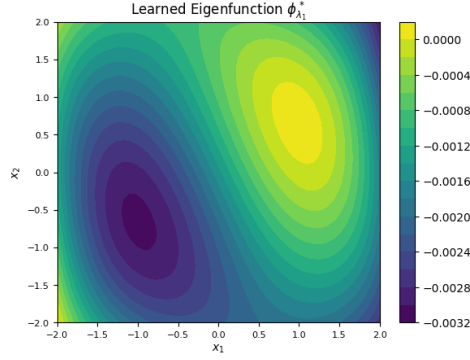


Figure 5: Learned $\phi_{\lambda_1}^*$

where the potential function V is given by

$$V(x) = x^\top P x + e^{-(x_1 - x_2)^2}, \quad (33)$$

where $P = \begin{pmatrix} 0.2 & 0.1 & 0.05 \\ 0.1 & 0.3 & 0.05 \\ 0.05 & 0.05 & 0.2 \end{pmatrix}$ is a positive definite matrix. The system admits an unstable equilibrium at the origin and two stable minima at $x = (0.90, -0.73, 0.14)$ and $x = (-0.90, 0.73, 0.14)$. We first compute Jacobian matrix of $-\frac{\partial V}{\partial x}$ at $x = 0$ which has three real eigenvalues, i.e., 3.70, -0.29, and -0.81. To construct $\phi_\lambda(x)$, we solve (17) over the domain $[-2, 2] \times [-2, 2] \times [-2, 2]$ by sampling 3379 points and use the Gaussian kernel $K(x_1, x_2) = \exp\left(-\frac{(x_1 - x_2)^2}{2 \times 1.1^2}\right)$. To visualize the result, we plot the level curve of $\phi_\lambda(x)$ with the unstable eigenvalue $\lambda = 3.70$ with a fixed $z = 0.57$. As shown in Figure 6, the level curve reveals two regions of attraction centered at the local minima of $V(x)$, i.e., x_1, x_2 .

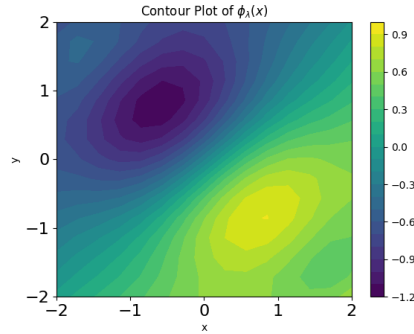


Figure 6: Learned $\phi_{\lambda_1}^*$

6 Code

The code for this paper can be found at <https://github.com/jonghyeon1998/Koopman>

7 Conclusion

In this paper, we have introduced a novel kernel-based method for approximating the principal eigenfunctions of the Koopman operator, offering a computationally efficient alternative to directly calculating the operator itself. By leveraging the decomposition of the eigenfunctions into linear and nonlinear components, we have shown that the linear part corresponds to the local linear dynamics of the system, while the nonlinear part can be obtained through kernel methods.

Our approach not only makes the computation of Koopman eigenfunctions more tractable but also enhances the ability to analyze complex dynamical systems by providing valuable insights into their long-term behavior. Overall, the kernel-based method for the construction of eigenfunctions of the Koopman operator presented here represents a significant step toward bridging the gap between linear and nonlinear dynamics within a rigorous mathematical framework.

Acknowledgement

GS is a member of INdAM-GNCS, and his work was partially supported by the project “Data-driven discovery and control of multi-scale interacting artificial agent system” funded by the program Next-GenerationEU - National Recovery and Resilience Plan (NRRP) – CUP H53D23008920001. HO and JL acknowledge support from the Air Force Office of Scientific Research under MURI award number FA9550-20-1-0358 (Machine Learning and Physics-Based Modeling and Simulation) and the Department of Energy under the MMICCs SEA-CROGS award. BH acknowledges support from NSF EPCN-2031570, the Air Force Office of Scientific Research (award number FA9550-21-1-0317) and the Department of Energy (award number SA22-0052-S001). HO is grateful for support from a Department of Defense Vannevar Bush Faculty Fellowship.

References

- [1] H. Kantz and T. Schreiber, *Nonlinear Time Series Analysis*. USA: Cambridge University Press, 1997.
- [2] M. Casdagli, “Nonlinear prediction of chaotic time series,” *Physica D: Nonlinear Phenomena*, vol. 35, no. 3, pp. 335 – 356, 1989. [Online]. Available: <http://www.sciencedirect.com/science/article/pii/0167278989900742>

- [3] J. L. Hudson, M. Kube, R. A. Adomaitis, I. G. Kevrekidis, A. S. Lapedes, and R. Farber, “Nonlinear signal processing and system identification: Applications to time series from electrochemical reactions,” *Chemical Engineering Science*, vol. 45, no. 8, pp. 2075–2081, 1990. [Online]. Available: <https://www.sciencedirect.com/science/article/pii/000925099080079T>
- [4] R. Rico-Martinez, K. Krischer, I. Kevrekidis, M. Kube, and J. Hudson, “Discrete-vs. continuous-time nonlinear signal processing of cu electrodisolution data,” *Chemical Engineering Communications*, vol. 118, no. 1, pp. 25–48, 1992.
- [5] O. Grandstrand, “Nonlinear system identification using neural networks: dynamics and instabilities,” in *Neural Networks for Chemical Engineers*, A. B. Bulsari, Ed. Elsevier: Elsevier, 1995, ch. 16, pp. 409–442.
- [6] R. González-García, R. Rico-Martínez, and I. Kevrekidis, “Identification of distributed parameter systems: A neural net based approach,” *Computers and Chemical Engineering*, vol. 22, pp. S965–S968, 1998, european Symposium on Computer Aided Process Engineering-8. [Online]. Available: <https://www.sciencedirect.com/science/article/pii/S0098135498001914>
- [7] A. Chattopadhyay, P. Hassanzadeh, K. V. Palem, and D. Subramanian, “Data-driven prediction of a multi-scale lorenz 96 chaotic system using a hierarchy of deep learning methods: Reservoir computing, ann, and RNN-LSTM,” *CoRR*, vol. abs/1906.08829, 2019. [Online]. Available: <http://arxiv.org/abs/1906.08829>
- [8] S. L. Brunton, J. L. Proctor, and J. N. Kutz, “Discovering governing equations from data by sparse identification of nonlinear dynamical systems,” *Proceedings of the National Academy of Sciences*, vol. 113, no. 15, pp. 3932–3937, 2016. [Online]. Available: <https://www.pnas.org/content/113/15/3932>
- [9] J. Pathak, Z. Lu, B. R. Hunt, M. Girvan, and E. Ott, “Using machine learning to replicate chaotic attractors and calculate lyapunov exponents from data,” *Chaos: An Interdisciplinary Journal of Nonlinear Science*, vol. 27, no. 12, p. 121102, 2017. [Online]. Available: <https://doi.org/10.1063/1.5010300>
- [10] A. Nielsen, *Practical Time Series Analysis: Prediction with Statistics and Machine Learning*. O’Reilly Media, 2019.
- [11] H. Abarbanel, *Analysis of Observed Chaotic Data*, ser. Institute for Nonlinear Science. Springer New York, 2012.
- [12] G. Pillonetto, M. H. Quang, and A. Chiuso, “A New Kernel-Based Approach for Nonlinear System Identification,” *IEEE Transactions on Automatic Control*, vol. 56, no. 12, pp. 2825–2840, Dec. 2011.

- [13] W.-X. Wang, R. Yang, Y.-C. Lai, V. Kovanis, and C. Grebogi, “Predicting Catastrophes in Nonlinear Dynamical Systems by Compressive Sensing,” *Physical Review Letters*, vol. 106, no. 15, p. 154101, Apr. 2011.
- [14] S. L. Brunton, J. L. Proctor, and J. N. Kutz, “Discovering governing equations from data by sparse identification of nonlinear dynamical systems,” *Proceedings of the National Academy of Sciences*, vol. 113, no. 15, pp. 3932–3937, 2016.
- [15] B. Lusch, J. N. Kutz, and S. L. Brunton, “Deep learning for universal linear embeddings of nonlinear dynamics,” *Nature Communications*, vol. 9, no. 1, p. 4950, Dec. 2018.
- [16] J. L. Callahan, J. V. Koch, B. W. Brunton, J. N. Kutz, and S. L. Brunton, “Learning dominant physical processes with data-driven balance models,” *Nature Communications*, vol. 12, no. 1, p. 1016, Dec. 2021.
- [17] A. A. Kaptanoglu, K. D. Morgan, C. J. Hansen, and S. L. Brunton, “Physics-constrained, low-dimensional models for magnetohydrodynamics: First-principles and data-driven approaches,” *Physical Review E*, vol. 104, no. 1, p. 015206, Jul. 2021.
- [18] J. N. Kutz and S. L. Brunton, “Parsimony as the ultimate regularizer for physics-informed machine learning,” *Nonlinear Dynamics*, Jan. 2022.
- [19] B. O. Koopman and J. v. Neumann, “Dynamical systems of continuous spectra,” *Proceedings of the National Academy of Sciences*, vol. 18, no. 3, pp. 255–263, 1932.
- [20] I. Mezić, “Spectral properties of dynamical systems, model reduction and decompositions,” *Nonlinear Dynamics*, vol. 41, no. 1, pp. 309–325, 2005.
- [21] A. Mauroy and I. Mezić, “Global stability analysis using the eigenfunctions of the koopman operator,” *IEEE Transactions on Automatic Control*, vol. 61, no. 11, pp. 3356–3369, 2016.
- [22] B. Umathe and U. Vaidya, “Spectral koopman method for identifying stability boundary,” *IEEE Control Systems Letters*, 2023.
- [23] A. R. Matavalam, B. Hou, H. Choi, S. Bose, and U. Vaidya, “Data-driven transient stability analysis using the koopman operator,” *International Journal of Electrical Power & Energy Systems*, vol. 162, p. 110307, 2024.
- [24] U. Vaidya, “Spectral analysis of koopman operator and nonlinear optimal control,” in *2022 IEEE 61st Conference on Decision and Control (CDC)*. IEEE, 2022, pp. 3853–3858.
- [25] —, “When Koopman meets Hamilton and Jacobi,” *In preprint*, 2024.

- [26] S. A. Deka, S. S. Narayanan, and U. Vaidya, “Path-integral formula for computing koopman eigenfunctions,” in *2023 62nd IEEE Conference on Decision and Control (CDC)*. IEEE, 2023, pp. 6641–6646.
- [27] M. Colbrook, “The foundations of infinite-dimensional spectral computations,” Ph.D. dissertation, University of Cambridge, 2020.
- [28] M. O. Williams, I. G. Kevrekidis, and C. W. Rowley, “A data-driven approximation of the koopman operator: Extending dynamic mode decomposition,” *Journal of Nonlinear Science*, vol. 25, no. 6, pp. 1307–1346, 2015.
- [29] S. Klus, F. Nüske, S. Peitz, J.-H. Niemann, C. Clementi, and C. Schütte, “Data-driven approximation of the Koopman generator: Model reduction, system identification, and control,” *Physica D: Nonlinear Phenomena*, vol. 406, p. 132416, 2020.
- [30] B. Peherstorfer, S. L. Brunton, and J. N. Kutz, “Data-driven koopman operators for model reduction and control of systems with symmetries,” *SIAM Journal on Applied Dynamical Systems*, vol. 19, no. 3, pp. 1894–1920, 2020.
- [31] S. Klus, F. Nüske, P. Koltai, I. G. Kevrekidis, C. Schütte, and C. Clementi, “Kernel-based dynamic mode decomposition,” *Journal of Computational Dynamics*, vol. 2, no. 2, pp. 247–265, 2015.
- [32] S. Das and D. Giannakis, “Koopman spectra in reproducing kernel hilbert spaces,” *Applied and Computational Harmonic Analysis*, vol. 49, no. 2, pp. 573–607, 2020. [Online]. Available: <https://www.sciencedirect.com/science/article/pii/S1063520320300427>
- [33] B. Hou, S. Sanjari, N. Dahlin, S. Bose, and U. Vaidya, “Sparse learning of dynamical systems in RKHS: An operator-theoretic approach,” in *International Conference on Machine Learning*. PMLR, 2023, pp. 13 325–13 352.
- [34] I. Ishikawa, Y. Hashimoto, M. Ikeda, and Y. Kawahara, “Koopman operators with intrinsic observables in rigged reproducing kernel hilbert spaces,” 2024. [Online]. Available: <https://arxiv.org/abs/2403.02524>
- [35] F. Cucker and S. Smale, “On the mathematical foundations of learning,” *Bulletin of the American mathematical society*, vol. 39, no. 1, pp. 1–49, 2002.
- [36] Y. Chen, B. Hosseini, H. Owhadi, and A. M. Stuart, “Solving and learning nonlinear pdes with gaussian processes,” *Journal of Computational Physics*, vol. 447, 2021.
- [37] P. Batlle, Y. Chen, B. Hosseini, H. Owhadi, and A. M. Stuart, “Error analysis of kernel/gp methods for nonlinear and parametric pdes,” *Journal of Computational Physics*, vol. 520, p. 113488, 2025.

- [38] H. Owhadi, “Computational Graph Completion,” *Research in the Mathematical Sciences*, vol. 9(2), no. 27, 2021. [Online]. Available: <https://arxiv.org/abs/2110.10323>
- [39] T. Bourdais, P. Batlle, X. Yang, R. Baptista, N. Rouquette, and H. Owhadi, “Codiscovering graphical structure and functional relationships within data: A gaussian process framework for connecting the dots,” *Proceedings of the National Academy of Sciences*, vol. 121, no. 32, p. e2403449121, 2024.
- [40] B. Haasdonk, B. Hamzi, G. Santin, and D. Wittwar, “Greedy kernel methods for center manifold approximation,” *Proc. of ICOSAHOM 2018, International Conference on Spectral and High Order Methods*, vol. 427, no. 1, 2018, <https://arxiv.org/abs/1810.11329>.
- [41] —, “Kernel methods for center manifold approximation and a weak data-based version of the center manifold theorems,” *Physica D*, 2021.
- [42] P. Giesl, B. Hamzi, M. Rasmussen, and K. Webster, “Approximation of Lyapunov functions from noisy data,” *Journal of Computational Dynamics*, vol. 7, pp. 57–81, 2019, <https://arxiv.org/abs/1601.01568>.
- [43] B. Hamzi and H. Owhadi, “Learning dynamical systems from data: A simple cross-validation perspective, Part I: Parametric Kernel Flows,” *Physica D: Nonlinear Phenomena*, vol. 421, p. 132817, 2021. [Online]. Available: <https://www.sciencedirect.com/science/article/pii/S0167278920308186>
- [44] B. Hamzi and F. Colonius, “Kernel methods for the approximation of discrete-time linear autonomous and control systems,” *SN Applied Sciences*, vol. 1, no. 7, pp. 1–12, 2019.
- [45] S. Klus, F. Nuske, and B. Hamzi, “Kernel-based approximation of the Koopman generator and Schrödinger operator,” *Entropy*, vol. 22, 2020, <https://www.mdpi.com/1099-4300/22/7/722>.
- [46] R. Alexander and D. Giannakis, “Operator-theoretic framework for forecasting nonlinear time series with kernel analog techniques,” *Physica D: Nonlinear Phenomena*, vol. 409, p. 132520, 2020. [Online]. Available: <http://www.sciencedirect.com/science/article/pii/S016727891930377X>
- [47] A. B. S. K. B. H. P. Koltai, and C. Schutte, “Dimensionality reduction of complex metastable systems via kernel embeddings of transition manifold,” *Journal of Nonlinear Science*, vol. 31(3), 2019.
- [48] J. Bouvrie and B. Hamzi, “Empirical estimators for stochastically forced nonlinear systems: Observability, controllability and the invariant measure,” *Proc. of the 2012 American Control Conference*, pp. 294–301, 2012, <https://arxiv.org/abs/1204.0563v1>.

- [49] —, “Kernel methods for the approximation of nonlinear systems,” *SIAM J. Control and Optimization*, 2017, <https://arxiv.org/abs/1108.2903>.
- [50] —, “Kernel methods for the approximation of some key quantities of nonlinear systems,” *Journal of Computational Dynamics*, vol. 1, 2017, <http://arxiv.org/abs/1204.0563>.
- [51] B. Hamzi, C. Kuehn, and S. Mohamed, “A note on kernel methods for multiscale systems with critical transitions,” *Mathematical Methods in the Applied Sciences*, vol. 42, no. 3, pp. 907–917, 2019. [Online]. Available: <https://onlinelibrary.wiley.com/doi/abs/10.1002/mma.5394>
- [52] L. Yang, X. Sun, B. Hamzi, H. Owhadi, and N. Xie, “Learning dynamical systems from data: A simple cross-validation perspective, Part V: Sparse Kernel Flows for 132 chaotic dynamical systems,” *Physica D*, vol. 460, 2022.
- [53] L. Yang, B. Hamzi, Y. Kevrekidis, H. Owhadi, X. Sun, and N. Xie, “Learning dynamical systems from data: A simple cross-validation perspective, Part VI: Hausdorff-metric based Kernel Flows to learn Attractors and Invariant Sets,” *Physica D*, 2023.
- [54] B. Hou, A. R. R. Matavalam, S. Bose, and U. Vaidya, “Propagating uncertainty through system dynamics in reproducing kernel hilbert space,” *Physica D: Nonlinear Phenomena*, p. 134168, 2024.
- [55] J. Lee, B. Hamzi, Y. Kevrekidis, and H. Owhadi, “Gaussian processes simplify differential equations,” September 2024. [Online]. Available: https://www.researchgate.net/publication/383680496_Gaussian_Processes_Simplify_Differential_Equations
- [56] D. Lengyel, B. Hamzi, H. Owhadi, and P. Parpas, “Kernel sum of squares for data adapted kernel learning of dynamical systems from data: A global optimization approach,” *arXiv preprint arXiv:2408.06465*, 2024. [Online]. Available: <https://www.arxiv.org/pdf/2408.06465>
- [57] G. Santin and B. Haasdonk, “Kernel methods for surrogate modeling,” *System and Data-Driven Methods and Algorithms*, 2019, <https://arxiv.org/abs/1907.105566>.
- [58] M. J. Colbrook, I. Mezić, and A. Stepanenko, “Limits and powers of koopman learning,” *arXiv preprint arXiv:2407.06312*, 2024.
- [59] P. Bevanda, M. Beier, A. Lederer, S. Sosnowski, E. Hüllermeier, and S. Hirche, “Koopman kernel regression,” *Advances in Neural Information Processing Systems*, vol. 36, 2024.

- [60] I. Mezić, “Spectrum of the koopman operator, spectral expansions in functional spaces, and state-space geometry,” *Journal of Nonlinear Science*, vol. 30, no. 5, pp. 2091–2145, 2020.
- [61] —, “Koopman operator, geometry, and learning of dynamical systems,” *Not. Am. Math. Soc.*, vol. 68, no. 7, pp. 1087–1105, 2021.
- [62] A. Lasota and M. C. Mackey, *Chaos, Fractals, and Noise: Stochastic Aspects of Dynamics*. New York: Springer-Verlag, 1994.
- [63] M. Budišić, R. Mohr, and I. Mezić, “Applied koopmanism,” *Chaos: An Interdisciplinary Journal of Nonlinear Science*, vol. 22, no. 4, p. 047510, 2012.
- [64] V. Arnold, *Geometrical Methods in the Theory of Ordinary Differential Equations*. Springer Verlag, 2012.
- [65] N. Aronszajn, “Theory of reproducing kernels,” *Transactions of the American Mathematical Society*, vol. 68, no. 3, pp. 337–404, 1950. [Online]. Available: <http://dx.doi.org/10.2307/1990404>
- [66] H. Owhadi and C. Scovel, *Operator-Adapted Wavelets, Fast Solvers and Numerical Homogenization: From a Game Theoretic Approach to Numerical Approximation and Algorithm Design*. Cambridge Monographs on Applied and Computational Mathematics. Cambridge University Press, 2019.
- [67] F. J. Narcowich, J. D. Ward, and H. Wendland, “Sobolev bounds on functions with scattered zeros, with applications to radial basis function surface fitting,” *Mathematics of Computation*, vol. 74, no. 250, pp. 743–763, 2005.